Abdominal Radiology

Cardiac-induced liver deformation as a measure of liver stiffness using dynamic imaging without magnetisation tagging – preclinical proof-of-concept, clinical translation, reproducibility and feasibility in patients with cirrhosis

--Manuscript Draft--

Manuscript Number:	AIMA-D-21-00246R1
Full Title:	Cardiac-induced liver deformation as a measure of liver stiffness using dynamic imaging without magnetisation tagging – preclinical proof-of-concept, clinical translation, reproducibility and feasibility in patients with cirrhosis
Article Type:	Original research
Corresponding Author:	Manil D Chouhan University College London London, London UNITED KINGDOM
Corresponding Author Secondary Information:	
Corresponding Author's Institution:	University College London
Corresponding Author's Secondary Institution:	
First Author:	Manil D Chouhan, MRCS FRCR PhD
First Author Secondary Information:	
Order of Authors:	Manil D Chouhan, MRCS FRCR PhD
	Heather E Fitzke, PhD
	Alan Bainbridge, PhD
	David Atkinson, PhD
	Steve Halligan, MRCP FRCR MD PhD
	Nathan Davies, PhD
	Mark F Lythgoe, PhD
	Rajeshwar P Mookerjee, FRCP PhD
	Alex Menys, PhD
	Stuart A Taylor, MRCP FRCR MD
Order of Authors Secondary Information:	
Funding Information:	Wellcome Trust (WT092186) — Dr Manil D Chouhan UCLH Biomedical Research Centre — Professor Stuart A Taylor
Abstract:	Purpose MR elastography and magnetisation-tagging use liver stiffness (LS) measurements to diagnose fibrosis but require physical drivers, specialist sequences and post-processing. Here we evaluate non-rigid registration of dynamic two-dimensional cine MRI images to measure cardiac-induced liver deformation (LD) as a measure of LS by (i) assessing preclinical proof-of-concept, (ii) clinical reproducibility and inter-reader variability, (iii) the effects of hepatic haemodynamic changes and (iv) feasibility in patients with cirrhosis. Methods Sprague-Dawley rats (n=21 bile duct ligated (BDL), n=17 sham-operated controls) and

	fasted patients with liver cirrhosis (n=11) and healthy volunteers (HVs, n=10) underwent spoiled gradient-echo short-axis cardiac cine MRI studies at 9.4T (rodents) and 3.0T (humans). LD measurements were obtained from intrahepatic sub-cardiac regions-of-interest close to the diaphragmatic margin. One-week reproducibility and prandial-stress induced haemodynamic changes were assessed in healthy volunteers. Results Normalised LD was higher in BDL (1.304±0.062) compared with sham-operated rats (1.058±0.045, P=0.0031). HV seven-day reproducibility Bland-Altman (BA) limits-of-agreement (LoAs) were ±0.028 a.u. and inter-reader variability BA LoAs were ±0.030 a.u.. Post-prandial LD increases were non-significant (+0.0083±0.0076 a.u., P=0.3028) and uncorrelated with PV flow changes (r=0.42, p=0.2219). LD measurements successfully obtained from all patients were not significantly higher in cirrhotics (0.102±0.0099 a.u.) compared with HVs (0.080±0.0063 a.u., P=0.0847). Conclusion Cardiac-induced LD is a conceptually reasonable approach from preclinical studies, measurements demonstrate good reproducibility and inter-reader variability, are less likely to be affected by hepatic haemodynamic changes and are feasible in patients with cirrhosis.
Response to Reviewers:	Detailed in-line response to the reviewer comments can be found in the supplementary material, uploaded in a separate word document.

Title:

Cardiac-induced liver deformation as a measure of liver stiffness using dynamic imaging without magnetisation tagging – preclinical proof-of-concept, clinical translation, reproducibility and feasibility in patients with cirrhosis

Author information:

Manil D Chouhan
Qualifications: MRCS FRCR PhD
Affiliations: University College London (UCL) Centre for Medical Imaging, Division of Medicine, UCL, London, UK

Heather E Fitzke
Qualifications: PhD
Affiliations: University College London (UCL) Centre for Medical Imaging, Division of Medicine, UCL, London, UK

Queen Mary University of London (QMUL) Wingate Institute of Neurogastroenterology, Neuroscience & Trauma, London UK

Alan Bainbridge
Qualifications: PhD
Affiliations: Department of Medical Physics, University College London Hospitals NHS Trust, London, UK.

David Atkinson
Qualifications: PhD
Affiliations: University College London (UCL) Centre for Medical Imaging, Division of Medicine, UCL, London, UK

Steve Halligan
Qualifications: MRCP FRCR MD PhD
Affiliations: University College London (UCL) Centre for Medical Imaging, Division of Medicine, UCL, London, UK

Nathan Davies
Qualifications: PhD
Affiliations: University College London (UCL) Institute for Liver and Digestive Health, Division of Medicine, UCL, London, UK

Mark F Lythgoe
Qualifications: PhD
Affiliations: University College London (UCL) Centre for Advanced Biomedical Imaging, Division of Medicine, UCL, London, UK

Rajeshwar P Mookerjee
Qualifications: FRCP PhD
Affiliations: University College London (UCL) Institute for Liver and Digestive Health, Division of Medicine, UCL, London, UK

Alex Menys
Qualifications: PhD
Affiliations: University College London (UCL) Centre for Medical Imaging, Division of Medicine, UCL, London, UK

Motilent, London, UK

Stuart A Taylor
Qualifications: MRCP FRCR MD
Affiliations: University College London (UCL) Centre for Medical Imaging, Division of Medicine, UCL, London, UK

Corresponding author information:

Name: Manil Dinesh Chouhan
Address: UCL Centre for Medical Imaging
2nd Floor Charles Bell House

43-45 Foley Street
W1W 7TS
London
United Kingdom
Email: m.chouhan@ucl.ac.uk
Telephone: +44 207 679 8156
ORCID ID: 0000-0001-5903-1002

Abstract:

Purpose:

MR elastography and magnetisation-tagging use liver stiffness (LS) measurements to diagnose fibrosis but require physical drivers, specialist sequences and post-processing. Here we evaluate non-rigid registration of dynamic two-dimensional cine MRI images to measure cardiac-induced liver deformation (LD) as a measure of LS by (i) assessing preclinical proof-of-concept, (ii) clinical reproducibility and inter-reader variability, (iii) the effects of hepatic haemodynamic changes and (iv) feasibility in patients with cirrhosis.

Methods:

Sprague-Dawley rats (n=21 bile duct ligated (BDL), n=17 sham-operated controls) and fasted patients with liver cirrhosis (n=11) and healthy volunteers (HVs, n=10) underwent spoiled gradient-echo short-axis cardiac cine MRI studies at 9.4T (rodents) and 3.0T (humans). LD measurements were obtained from intrahepatic sub-cardiac regions-of-interest close to the diaphragmatic margin. One-week reproducibility and prandial-stress induced haemodynamic changes were assessed in healthy volunteers.

Results:

Normalised LD was higher in BDL (1.304±0.062) compared with sham-operated rats (1.058±0.045, P=0.0031). HV seven-day reproducibility Bland-Altman (BA) limits-of-agreement (LoAs) were ±0.028 a.u. and inter-reader variability BA LoAs were ±0.030 a.u.. Post-prandial LD increases were non-significant (+0.0083±0.0076 a.u., P=0.3028) and uncorrelated with PV flow changes (r=0.42, p=0.2219). LD measurements successfully obtained from all patients were not significantly higher in cirrhotics (0.102±0.0099 a.u.) compared with HVs (0.080±0.0063 a.u., P=0.0847).

Conclusion:

Cardiac-induced LD is a conceptually reasonable approach from preclinical studies, measurements demonstrate good reproducibility and inter-reader variability, are ~~robust to~~less likely to be affected by hepatic haemodynamic changes and are feasible in patients with cirrhosis.

Commented [MC1]: R1.1

Keywords:

liver fibrosis, cirrhosis, MRI, elasticity imaging techniques, organ motion

Declarations:

Funding:

Wellcome Trust Clinical Research Training Fellowship (grant WT092186)
National Institute of Health Research University College London Hospitals Biomedical Research Centre

Conflicts of interest/competing interests:

Manil D Chouhan – no relevant conflicts of interest or competing interests to declare
Heather E Fitzke - BBBSRC funded work placements with Motilent Ltd in 2018 & 2020 (BB/S508019/1). No other relevant conflicts of interest or competing interests to declare.
Alan Bainbridge – no relevant conflicts of interest or competing interests to declare
David Atkinson – no relevant conflicts of interest or competing interests to declare
Steve Halligan – no relevant conflicts of interest or competing interests to declare
Nathan Davies – no relevant conflicts of interest or competing interests to declare
Mark F Lythgoe – no relevant conflicts of interest or competing interests to declare
Rajeshwar P Mookerjee – no relevant conflicts of interest or competing interests to declare
Alex Menys – is the CEO of Motilent. No other relevant conflicts of interest or competing interests to declare.

Stuart A Taylor - has share options in Motilent and is a consultant at Alimentiv. No other relevant conflicts of interest or competing interests to declare.

Availability of data and material:
The authors confirm that the data supporting the findings of this study are available within the article. Raw data were generated at the UCL Centre for Medical Imaging/UCL Centre for Advanced Biomedical Imaging. Derived data supporting the findings of this study are available from the corresponding author on request.

Code availability:
Cardiac cine MRI data was analysed using GIQuant® (Motilent, London, UK).

Authors contributions:
Manil D Chouhan – guarantor of integrity of the entire study, study concepts and design, literature research, clinical studies, experimental pre-clinical studies, data-analysis, statistical analysis, manuscript preparation, manuscript editing
Heather E Fitzke – study concepts and design, experimental pre-clinical studies, data-analysis, manuscript editing
Alan Bainbridge – clinical studies, experimental pre-clinical studies, data-analysis
David Atkinson - clinical studies, experimental pre-clinical studies, data analysis, manuscript editing
Steve Halligan – statistical analysis, manuscript editing
Nathan Davies – experimental preclinical studies
Mark F Lythgoe - experimental preclinical studies
Rajeshwar P Mookerjee – clinical studies, experimental preclinical studies, manuscript editing
Alex Menys – study concepts and design, experimental pre-clinical studies, clinical studies, data-analysis, manuscript editing
Stuart A Taylor – study concepts and design, manuscript editing

Ethics approval:
Preclinical - approval obtained from the Animal Care Ethical Committee of University College London.
Clinical - Research Ethics Committee (Joint RNOH/IOMS, reference number 08/H0724/35) approval was obtained.

Consent to participate:
Written consent obtained from all clinical study participants.

Consent for publication:
Written consent obtained from all clinical study participants, with implied consent from all authors.

Specific Remarks:
Not applicable

Introduction

Cirrhosis and chronic liver disease remain major causes of global morbidity and mortality[1]. Liver fibrosis, a precursor to cirrhosis and common pathological phenotype of liver disease is characterised by tissue accumulation of extracellular matrix proteins and remodelling[2]. Diagnosing the presence and severity of liver fibrosis – particularly in early-stage liver disease – can direct treatment and lifestyle changes that may enable recovery. Gold standard fibrosis measurements however require invasive biopsy with procedural morbidity and occasional mortality, rendering screening for early disease and repeated measurements unfeasible. Biopsy samples are also small and prone to sampling error and significant inter-/intra-observer variability[3, 4].

In response to chronic injury, fibrotic processes progressively alter the biomechanical properties of the liver including tissue viscosity, elasticity and stiffness. These form the basis of modern non-invasive biomechanical imaging methods to measure fibrosis [5]. By measuring tissue response to an applied physical stress, biomechanical imaging methods such as ultrasound and MR elastography (MRE) measure liver stiffness as a biomarker of fibrosis. US-based elastography methods are most widely used but, like biopsy, only sample a small liver tissue volumes, often blindly (in the case of transient elastrography)[6, 7]. MRE potentially maps whole liver tissue stiffness, but requires an external driver strapped to the abdomen to induce mechanical waves. Modified phase-contrast MRI sequences are then used to map tissue stiffness, but the driver may cause discomfort and measurements can be compromised in obese patients by field inhomogeneities particularly at higher field strength and in patients with hepatic iron-overload[8, 9].

MR strain imaging is a more recent biomechanical imaging method based on liver deformation caused by physiological strain caused by cardiac or respiratory motion, using either cine magnetisation tagging or strain-encoding imaging[10–12]. Most studies have used cardiac-induced liver deformation with encouraging early results demonstrating differences between patients with varying stages of histologically proven fibrosis[13, 14] and disease severity[15]. While these approaches avoid additional hardware and mechanical drivers, both require specialist sequences and post-processing that are not widely available.

Non-rigid registration of dynamic two-dimensional cine MR images has been used to successfully quantify small bowel motility[16] and vocal cord motion[17], and can assess Crohn's disease and treatment response[18]. In tissue such as the liver, it is possible that deformation reflects tissue stiffness, potentially yielding a more readily available biomarker if cirrhosis that could be readily obtained from widely available MR sequences. We propose using non-rigid registration of two-dimensional dynamic cine MR images of the liver to measure cardiac-induced liver deformation (LD). Here we (a) evaluate LD measurement in a preclinical rodent model as a proof-of-concept,

before clinical translation to normal volunteers, with (b) assessment of reproducibility, (c) inter-reader variability, (d) the effects of hepatic haemodynamic changes using prandial stress (as haemodynamic changes could induce changes in tissue elasticity) and finally (e) feasibility in cirrhotic patients.

Materials and Methods

Preclinical proof-of-concept

Subjects and preparation

Experiments were conducted using <blinded> guidelines under <blinded>, with approval from the Animal Care Ethical Committee of <blinded>. Healthy male Sprague-Dawley rats (<blinded>) with normal liver function (weight 250-300g) underwent either sham laparotomy or bile duct ligation[19]. Animals were maintained for 4-5 weeks after the procedure to enable chronic liver disease to develop in BDL rats as verified by previously reported histopathological and phenotypic changes at our institution[20].

Anaesthesia was induced and maintained at a constant level using isoflurane (2% in 1L O_2/min). A rectal probe (SA Instruments, New York, NY) was used to monitor core temperature, that was regulated while scanning using warm air and pipes with circulating warm water. A triple-electrode single-lead system and respiratory bellows (SA Instruments) were used for respiratory and cardiac monitoring respectively. All animal preparation was undertaken by the study coordinator (<blinded>, a radiology research fellow qualified in animal handling). Other imaging data derived from this same group of animals has been previously published[21].

Pre-clinical liver deformation measurement

Animals were scanned using a 9.4-T MRI system (Agilent Technologies, Oxford, England) with sequence parameters listed in table 1. Short-axis cardiac cine MRI studies were performed as described previously[21]. Cardiac and respiratory gated gradient-echo coronal images of the thorax and left-ventricular (LV) long-axis cardiac imaging were used to plan LV short-axis imaging. Spoiled gradient-echo imaging with 1 mm contiguous LV short-axis slices planned from the LV apex to the mitral valve orifice was undertaken using a 15˚ flip angle, 40x40 mm^2 field-of-view (FOV) and 128x64 (frequency encoding x phase encoding) matrix. Full LV coverage with data for at least 20 frames through the cardiac cycle (temporal resolution of approximately 7-9 milliseconds) was typically obtained in under 12 minutes. Data was analysed using deformation analysis software GIQuant® (Motilent, London, UK)[16, 22]. A single short-axis slice was selected mid-way between the cardiac apex and mitral valve and a single hepatic parenchymal region-of-interest (ROI) was drawn

close to the diaphragmatic margin and propagated automatically to other frames within the slice cine-loop. As cardiac cine MRI images were acquired with the primary objective of measuring dynamic changes in cardiac function in response to haemodynamic stress[21], imaging optimised to shorten acquisition times for LV segmentation was noted to have consistent noise artefact in the phase-encode direction (figure 1a and 1b). This was likely secondary to motion artefact introduced by prospective gating errors. Given the small deformation signal being measured, the noise had the potential to compromise deformation quantification, moreover the severity of the artefact varied between subjects. To account for this in a subject-specific way, a second extra-corporeal ROI of similar size to the parenchyma was placed within the imaged area outside of the body but parallel to the parenchymal ROI (figure 1a and 1b). ROIs were placed blinded to subject cohort via joint consensus between a radiology research fellow (<blinded>) and imaging scientist (<blinded>), both with >5 years' experience of abdominal imaging and use of GIQuant™ software. LD measured in arbitrary units (a.u.) was based on the standard deviation over time of each pixel's Jacobian determinant, summarised as the ROI mean[22]. To account for potential noise artefact, preclinical LD measurements were divided by the measurement obtained from the extra-corporeal ROI to calculate normalised LD (nLD, equation 1):

$$nLD\ (\text{unitless}) = \frac{\text{preclinical } LD\ (\text{a.u.})}{\text{Extra-corporeal ROI deformation (a.u.)}} \quad (1)$$

Human translation

Subjects and preparation

Research Ethics Committee approval was obtained and all participants provided informed written consent. Healthy volunteers were recruited by University campus advertisement. Exclusion criteria were (a) known contraindication to MRI, (b) any long-term medication (excluding oral contraceptives) and, (c) any previous history of liver or gastrointestinal disease. Patients with histologically confirmed cirrhosis undergoing invasive transjugular procedures for routine clinical care were recruited from hepatology outpatient clinics or elective transjugular intrahepatic portosystemic shunt (TIPSS) lists for refractory ascites, excepting participants who (a) had known MRI contraindication, (b) were unable to provide informed consent or, (c) were on specific treatment for portal hypertension (e.g. beta-blockers). All participants were asked to avoid caffeinated fluids and fast for six hours prior to MRI.

Clinical liver deformation measurement

Imaging was performed using a 3.0T scanner (Achieva, Philips Healthcare, Best, Netherlands) with a 16-channel body coil (SENSE XL-Torso, Philips Healthcare, Best, Netherlands) with sequence parameters listed in table 1. Short-axis cardiac cine MRI studies were planned using thoracic coronal and LV long-axis anatomical imaging. Images were obtained in expiratory breath-hold with pulse-oximetry signal used for cardiac gating. Spoiled gradient-echo imaging with 8 mm contiguous LV short-axis slices planned from the LV apex to the mitral orifice was undertaken using a 45° flip angle, 320x320 mm FOV and 256x256 matrix. Full LV coverage with data for approximately 30 cardiac cycle phases was typically obtained within 7 breath-holds. Data from a single short-axis slice selected mid-way between the cardiac apex and mitral valve was analysed using GIQuant™ by drawing a single ROI on the subdiaphragmatic hepatic parenchyma (avoiding vessels and ducts) and automatic propagation to other frames within the slice cine-loop (figure 1c and d). ROIs were placed independently by two imaging scientists blinded to clinical details (<blinded> and <blinded>), both with >5 years' experience of abdominal imaging and use of GIQuant™ software. LD was measured in arbitrary units (a.u.) as described above for preclinical subjects[22].

Hepatic haemodynamic assessment

Post-prandial stress was used to stimulate haemodynamic change. Phase-contrast MRI (PCMRI) measurements of portal venous (PV) flow were used to assess post-prandial haemodynamic response. Anatomical upper abdominal coronal steady-state free precession (SSFP) imaging was used to plan further SSFP imaging parallel to the PV, which together were used to plan two-dimensional PCMRI studies orthogonal to the vessel (sequence parameters listed in table 1). PV PCMRI studies were performed in expiratory breath-hold with pulse-oximetry based cardiac gating, using a velocity encoding setting (V_{enc}) of 40 cm/s, 10° flip angle, 5 mm slice thickness, 271x210 mm FOV and 336x336 matrix. Seven phases were obtained through the cardiac cycle and PCMRI measurements were performed in triplicate. Flow quantification was performed using Segment (Medviso, Lund, Sweden), with averaging of triplicate PV bulk flow measurements. Upper abdominal coronal SSFP imaging was used to estimate liver mass, with volumetric segmentation performed manually using Amira (Amira Resolve RT, Visage Imaging, Berlin, Germany) and assumption of 1.0 g/ml tissue density[23]. Triplicate PV bulk flow measurements normalised to estimated liver mass were averaged, with all PCMRI vessel and hepatic volumetric segmentation undertaken by the study coordinator (<blinded>).

Reproducibility, inter-reader variability and prandial stress studies

For reproducibility studies (n=8), subjects were fasted for 6 hours and scanned on the same scanner using the same MRI protocol 7 days later at a similar time of day. Assessment was based on measurements made by the more senior imaging scientist (<blinded>), blinded to baseline/reproducibility group or post-prandial state.

Independent clinical LD measurements from healthy volunteers at baseline (including reproducibility measurements) from both readers (<blinded> and <blinded>) were used for inter-reader variability studies. For prandial stress studies (n=10), healthy volunteers ingested 440 mls of oral Ensure Plus® (Abbot Laboratories, Illinois, USA) after the initial scan. MRI was then repeated 45-60 minutes after ingestion.

Statistical analysis

Statistical analyses used Prism (Graphpad Software Inc., version 6.01), with calculation of intra-class correlation coefficients using SPSS Statistics (IBM, version 26.0). Distribution normality was confirmed with Shapiro-Wilk testing. Comparisons between animal groups were undertaken with unpaired Student t-tests, with Welch's correction to account for group differences in standard deviation. Where appropriate (and indicated in the presented results), non-parametric Mann-Whitney U-tests were used for parameters that were not normally distributed. Clinical LD measurement reproducibility and inter-reader variability in healthy volunteers was assessed using Bland-Altman analysis with calculation of 95% limits-of-agreement (LoAs), intra-class correlation coefficient (ICC) estimation (using the mean of both measurements, absolute agreement and a two-way mixed-effects model) and within-subject Coefficient of Variation (CoV). The effects of prandial stress in healthy volunteers was assessed by comparing baseline and post-prandial PV flow and LD measurements using paired Student t-tests, with Welch's correction to account for group differences in standard deviation. Correlations between post-prandial change in PV flow and LD were assessed using Pearson's correlation coefficient. Baseline LD measurements in healthy volunteers were compared with liver disease patients using unpaired Student t-tests with Welch's correction. Data are expressed as means ± standard errors, with significance at the 5% threshold.

Results

Preclinical cohort and proof-of-concept

Similar weights were observed in both cohorts (250-300g) at baseline, but four weeks following surgery, wet liver mass was higher in BDL (31±1g, n=21) compared with sham-operated animals (15±1g, n=17, Mann-Whitney U-test, P<0.0001) but whole body weight was lower in BDL (413±9g)

compared with sham-operated animals (474±5g, P<0.0001). Measurements from five subjects were not possible due to wrap-around artefact resulting in insufficient area for appropriate placement of an extra-corporeal ROI or suboptimal image quality. Acceptable measurements were ultimately obtained from fifteen sham and eighteen BDL animals (figure 2a). Normalised LD was higher in BDL (1.304±0.062) compared with sham-operated rats (1.058±0.045, Mann-Whitney U-test, P=0.0031, table 2, figure 3).

Healthy volunteer cohort and clinical LD reproducibility and inter-reader variability

Ten healthy volunteers were recruited (5 males, 5 females, aged 28.6±1.6 years, figure 2b). Mean baseline LD was 0.080±0.0063 a.u. (table 2) and normal volunteer reproducibility studies (n=8) demonstrated a mean LD difference of 0.0043 a.u. with Bland-Altman 95% LoAs of ±0.028 a.u. (figure 4), ICC of 0.771 (P=0.008) and within-subject CoV of 12.7% after seven days.

Inter-reader variability studies using measurements obtained at baseline and after seven days (n=8 subjects, with 16 measurements made by each reader) demonstrated a mean LD difference of 0.0014 a.u. with Bland-Altman 95% LoAs of ±0.030 a.u. (figure 5), ICC of 0.787 (P<0.0001) and a CoV of 11.8% between both readers.

Prandial stress studies

All ten healthy volunteers participated in prandial stress studies. Post-prandial increases in PCMRI PV flow were observed (55.3±4.5 ml/min/100g in the fasted state compared with 106.0±3.9 ml/min/100g in the post-prandial state, mean difference +50.7±4.6 ml/min/100g, P<0.0001, figure 6a). Post-prandial LD was higher than in the fasted state, but this was not statistically significant (0.080±0.0063 a.u. in the fasted state compared with 0.088±0.0078 a.u. in the post-prandial state, mean difference +0.0083±0.0076 a.u., P=0.3028, table 2, figure 6b). No correlation was demonstrated between post-prandial change in LD and post-prandial change in PCMRI PV flow (r=0.42, p=0.2219, figure 6c).

Feasibility in patients with cirrhosis

Eleven patients participated in feasibility studies (10 males, 1 female, aged 53±3 years). Cirrhotic aetiologies included alcohol (n=8), non-alcoholic steatohepatitis cirrhosis (n=2) and hereditary haemochromatosis (n=1), with predominantly stable disease at the time of scanning (Child-Pugh score A=7, B=4) (figure 2c). LD measurements were obtained successfully from all patients. Although LD was higher in cirrhotic patients (0.102±0.0099 a.u.) compared with healthy volunteers (0.080±0.0063 a.u.), this difference was not statistically significant (P=0.0847, table 2, figure 7).

Discussion

We demonstrated the use of non-rigid registration of dynamic two-dimensional cardiac short-axis cine MR imaging to measure cardiac-induced liver deformation (LD). As a proof-of-concept we found that in a rat model of advanced liver disease, normalised LD measurements were significantly different to those obtained from control animals. Because imaging had been optimised for LV segmentation, varying levels of phase-encode direction noise artefact were addressed by normalising animal LD measurements to a second parallel extra-corporeal ROI. As this noise was not appreciable on clinical scans, human LD measurements were not normalised. Alternative magnetisation-tagging approaches to measure cardiac-induced liver motion have not reported preclinical data for validation/proof-of-concept but there have been several preclinical canine and porcine liver and splenic MRE studies demonstrating an association between stiffness, hepatic venous pressure gradient[24, 25] and fibrosis[26].

Following human translation, measured ICCs for LD reproducibility on the same scanner after 7 days in similar scanning conditions suggest measurement reliability, with reasonable within-subject CoVs. Repeatability studies (three measurements within the same scanning session) of respiratory-induced liver motion using magnetisation-tagging have reported comparable ICCs[10] and while formal reproducibility data for measurement of cardiac-induced liver motion using magnetisation-tagging has not been reported, a meta-analysis of MRE liver stiffness measurements across 274 patients has demonstrated a smaller within-subject CoV of 8%[27].

Inter-reader variability studies have also demonstrated good measurement reliability also with reasonable within-subject CoVs, despite the relatively small ROIs used and potential for noise contamination. Measured LD inter-reader variability ICCs, CoVs and Bland-Altman LoAs in this study were similar to LD reproducibility statistics, therefore suggesting that reader differences are unlikely to introduce variation outside of that expected from repeat measurement. Inter-reader variability was superior to that reported for cardiac-induced liver motion with magnetisation tagging (ICC of 0.584 and CoV of 29.7%)[13].

Post-prandial stress was used to stimulate haemodynamic change with the premise that this could induce changes in tissue elasticity and therefore LD. Although healthy volunteer post-prandial PV flow almost doubled, change in LD was not significant, and was much smaller than Bland-Altman LoAs for LD reproducibility and inter-reader variability. Furthermore, we found no statistically significant association between post-prandial change in PV flow and LD, although a general positive trend was noted between post-prandial change in LD and PV flow, suggesting that further studies would be needed before concluding that LD measurements are unlikely to be affected by

haemodynamic changes. Post-prandial changes in magnetisation-tagging derived measures of liver motion have not been reported, but small statistically significant increases in MRE liver stiffness and poor positive but significant correlations between change in MRE liver stiffness and PV flow have been demonstrated in the setting of a similar meal challenge[28]. This could suggest lower LD sensitivity to haemodynamic changes relative to MRE liver stiffness.

Finally, we demonstrated that LD measurements were feasible in patients with established liver disease and while LD increased relative to healthy volunteers, this difference was not statistically significant. This could reflect a type II error arising from the small sample size and larger scale studies are definitely needed to understand potential for disease severity stratification. It may also however reflect lower sensitivity in patients with milder more stable disease, as no data was collected in patients with decompensated cirrhosis, for example. Although sample size was small, demonstration of feasibility in patients with liver disease, including in the setting of iron-overload is an important strength. Patients often struggle with breath-holds, imaging is prone to motion artefact, and difficulties arising from the use of MRE external drivers or quantification errors in the setting of iron-overload are recognised limitations of alternative MR biomechanical imaging methods. We do acknowledge that only one patient in our sample had significant hepatic siderosis, so further work would be required to confirm if LD measurements are definitively robust in the setting of iron-overload. Interestingly, several studies measuring cardiac-induced liver motion with magnetisation-tagging have demonstrated reducing liver 'strain' with advancing liver disease[11, 13, 29], opposing our finding of increased normalised/absolute LD in the setting of liver disease. This may have arisen from methodological differences, and we postulate that higher LD values in liver disease may reflect greater sensitivity to increased translational motion (as a result of stiffer liver tissue), as opposed to greater elastic motion as seen in non-diseased liver (which strain methods are potentially more sensitive to). It is also worth noting that we studied a largely stable disease cohort (predominantly Child-Pugh A) – while this could account for a non-significantly higher patient LD, biomechanical properties of liver tissue are arguably more dependent upon the degree of fibrosis/cirrhosis severity rather than disease stability. Previous studies using magnetisation-tagging based measures of liver motion for example, were still able to demonstrate significantly different measurements in similarly sized patient cohorts with predominantly stable Child-Pugh A liver disease[29], suggesting that LD may have lower sensitivity.

Low sensitivity of LD measurements may reflect difficulties obtaining sufficient signal-to-noise, highlighted by our animal data and the use of small ROIs. Despite availability of data from the entirety of liver imaged within a single slice, the lack of signal further away from the left ventricle restricted measurements to a sub-cardiac location (negating the advantage of whole-liver coverage

and quantification) and conversely increasing the risk of noise contamination. It is worth noting that despite this, reproducibility and inter-reader variability were reasonable. Measured tissue deformation/motion is however directly related to the energy of applied stress, which likely varies between patients. For cardiac-induced motion, energy released by ventricular contraction is likely to vary in liver disease as cirrhotic cardiomyopathy is common[30]. . MRE for example, avoids this limitation by using an external driver so that stress is consistent between patients. Formal clinical translation is therefore likely to require use of a means of measuring the energy applied to the liver for normalisation of deformation measurements. It is worth noting that alternative approaches, including the tracking dynamic wave propagation through the liver during the cardiac cycle remain novel approaches that could potentially be used to calculate liver stiffness from cine MRI data.

Finally, despite these limitations, our findings remain relevant because they demonstrate the potential of LD in the assessment of liver disease. An important strength is the use of non-specialist MRI sequences, readily available on most scanners, simple to use, and easy for radiographers/technologists to acquire. We do recognise this benefit is partly mitigated by the need to use third party image registration software – in this work for example, we used a proprietary (commercial) image analysis tool to obtain measurements. Because measurements rely on signal-intensity based tissue deformation, measures are less likely to be affected by scanner vendors or field-strength. Avoiding additional hardware (such as a driver) decreases cost, increases acceptability and maximises patient comfort. Analyses are also an advantage, the GIQuant™ software used here is CE marked for clinical use (albeit in Crohn's Disease) and integrates directly with hospital PACS. GIQuant™ already includes respiratory motion correction features that may be used to exploit dynamic imaging through the respiratory cycle to derive a respiratory LD score.

This small-scale translational study has highlighted some important strengths and weaknesses of LD measurements, including the need for alternative approaches to the application and measurement of physical stress, and the need for appropriately powered patient studies. In summary, cardiac-induced liver deformation using non-rigid registration of dynamic two-dimensional cine MRI imaging is a conceptually reasonable approach from preclinical studies, LD measurements demonstrate good reproducibility and inter-reader variability, are robust to hepatic haemodynamic changes and are feasible in patients with liver disease.

References:

1. Sepanlou SG, Safiri S, Bisignano C, et al (2020) The global, regional, and national burden of cirrhosis by cause in 195 countries and territories, 1990–2017: a systematic analysis for the Global Burden of Disease Study 2017. Lancet Gastroenterol Hepatol 5:245–266. https://doi.org/10.1016/S2468-1253(19)30349-8
2. Pinzani M (2015) Pathophysiology of Liver Fibrosis. Dig Dis 33:492–497. https://doi.org/10.1159/000374096

3. Rockey DC, Caldwell SH, Goodman ZD, et al (2009) Liver biopsy. Hepatology 49:1017–1044. https://doi.org/10.1002/hep.22742
4. Bedossa P, Dargère D, Paradis V (2003) Sampling Variability of Liver Fibrosis in Chronic Hepatitis C. Hepatology 38:1449–1457. https://doi.org/10.1016/j.hep.2003.09.022
5. Chouhan MD, Lythgoe MF, Mookerjee RP, Taylor SA (2016) Vascular assessment of liver disease-towards a new frontier in MRI. Br J Radiol 89:. https://doi.org/10.1259/bjr.20150675
6. Sandrin L, Fourquet B, Hasquenoph JM, et al (2003) Transient elastography: a new noninvasive method for assessment of hepatic fibrosis. Ultrasound Med Biol 29:1705–1713
7. Nightingale K (2011) Acoustic Radiation Force Impulse (ARFI) Imaging: a Review. Curr Med Imaging Rev 7:328–339. https://doi.org/10.2174/157340511798038657
8. Wagner M, Corcuera-Solano I, Lo G, et al (2017) Technical Failure of MR Elastography Examinations of the Liver: Experience from a Large Single-Center Study. Radiology 284:401–412. https://doi.org/10.1148/radiol.2016160863
9. Kennedy P, Wagner M, Castéra L, et al (2018) Quantitative Elastography Methods in Liver Disease: Current Evidence and Future Directions. Radiology 286:738–763. https://doi.org/10.1148/radiol.2018170601
10. Watanabe H, Kanematsu M, Kitagawa T, et al (2010) MR elastography of the liver at 3 T with cine-tagging and bending energy analysis: Preliminary results. Eur Radiol 20:2381–2389. https://doi.org/10.1007/s00330-010-1800-0
11. Chung S, Breton E, Mannelli L, Axel L (2011) Liver stiffness assessment by tagged MRI of cardiac-induced liver motion. Magn Reson Med 65:949–955. https://doi.org/10.1002/mrm.22785
12. Harouni AA, Gharib AM, Osman NF, et al (2015) Assessment of liver fibrosis using fast strain-encoded MRI driven by inherent cardiac motion. Magn Reson Med 74:106–114. https://doi.org/10.1002/mrm.25379
13. Lefebvre T, Petitclerc L, Hébert M, et al (2020) MRI cine-tagging of cardiac-induced motion for noninvasive staging of liver fibrosis. J Magn Reson Imaging 51:1570–1580. https://doi.org/10.1002/jmri.26935
14. Ahmed Y, Hussein RS, Basha TA, et al (2020) Detecting liver fibrosis using a machine learning-based approach to the quantification of the heart-induced deformation in tagged MR images. NMR Biomed 33:. https://doi.org/10.1002/nbm.4215
15. Chung S, Kim KE, Park MS, et al (2014) Liver stiffness assessment with tagged MRI of cardiac-induced liver motion in cirrhosis patients. J Magn Reson Imaging 39:1301–1307. https://doi.org/10.1002/jmri.24260
16. Menys A, Taylor SA, Emmanuel A, et al (2013) Global small bowel motility: assessment with dynamic MR imaging. Radiology 269:443–450. https://doi.org/10.1148/radiol.13130151
17. Baki MM, Menys A, Atkinson D, et al (2016) Feasibility of vocal fold abduction and adduction assessment using cine-MRI. Eur Radiol. https://doi.org/10.1007/s00330-016-4341-3
18. Plumb AA, Menys A, Russo E, et al (2015) Magnetic resonance imaging-quantified small bowel motility is a sensitive marker of response to medical therapy in Crohn's disease. Aliment Pharmacol Ther 42:343–355. https://doi.org/10.1111/apt.13275
19. Harry D, Anand R, Holt S, et al (1999) Increased sensitivity to endotoxemia in the bile duct-ligated cirrhotic rat. Hepatology 30:1198–1205. https://doi.org/10.1002/hep.510300515
20. Davies NA, Hodges SJ, Pitsillides AA, et al (2006) Hepatic guanylate cyclase activity is decreased in a model of cirrhosis: A quantitative cytochemistry study. FEBS Lett 580:2123–2128. https://doi.org/10.1016/j.febslet.2006.02.080
21. Chouhan MD, Taylor SA, Bainbridge A, et al (2020) Haemodynamic changes in cirrhosis following terlipressin and induction of sepsis—a preclinical study using caval subtraction phase-contrast and cardiac MRI. Eur Radiol. https://doi.org/10.1007/s00330-020-07259-w
22. Odille F, Menys A, Ahmed A, et al (2012) Quantitative assessment of small bowel motility by nonrigid registration of dynamic MR images. Magn Reson Med 68:783–793.

https://doi.org/10.1002/mrm.23298
23. Kuo PC, Alfrey EJ, Li K, et al (1995) Magnetic resonance imaging-derived parameter of portal flow predicts volume-mediated pulmonary hypertension in liver transplantation candidates. Surgery 118:685–692. https://doi.org/10.1016/S0039-6060(05)80036-4
24. Nedredal GI, Yin M, McKenzie T, et al (2011) Portal hypertension correlates with splenic stiffness as measured with MR elastography. J Magn Reson Imaging 34:79–87. https://doi.org/10.1002/jmri.22610
25. Yin M, Kolipaka A, Woodrum DA, et al (2013) Hepatic and splenic stiffness augmentation assessed with MR elastography in an in vivo porcine portal hypertension model. J Magn Reson Imaging 38:809–815. https://doi.org/10.1002/jmri.24049
26. Huang SY, Abdelsalam ME, Harmoush S, et al (2014) Evaluation of liver fibrosis and hepatic venous pressure gradient with MR elastography in a novel swine model of cirrhosis. J Magn Reson Imaging 39:590–597. https://doi.org/10.1002/jmri.24189
27. Serai SD, Obuchowski NA, Venkatesh SK, et al (2017) Repeatability of MR Elastography of Liver: A Meta-Analysis. Radiology 285:92–100. https://doi.org/10.1148/radiol.2017161398
28. Jajamovich GH, Dyvorne H, Donnerhack C, Taouli B (2014) Quantitative liver MRI combining phase contrast imaging, elastography, and DWI: assessment of reproducibility and postprandial effect at 3.0 T. PLoS One 9:e97355. https://doi.org/10.1371/journal.pone.0097355
29. Mannelli L, Wilson GJ, Dubinsky TJ, et al (2012) Assessment of the liver strain among cirrhotic and normal livers using tagged MRI. J Magn Reson Imaging 36:1490–1495. https://doi.org/10.1002/jmri.23743
30. Wiese S, Hove JD, Bendtsen F, et al (2014) Cirrhotic cardiomyopathy: pathogenesis and clinical relevance. Nat Rev Gastroenterol Hepatol 11:177–186. https://doi.org/10.1038/nrgastro.2013.210

Figure captions:

Fig. 1: Short-axis cardiac cine images of representative slices and ROIs (yellow-dashed line) used for LD quantification in rats (a, b) and humans (c, d). Anatomical images are shown on the left (a, c) with overlaid deformation maps shown on the right (b, d). Note the presence of an additional extra-corporeal ROI parallel to the hepatic ROI used for normalisation to account for phase-encode direction noise artefact (a)

Fig. 2: Study cohorts

Fig. 3: Normalised Liver Deformation in sham control (■) and BDL rats (△)

Fig. 4: Seven-day reproducibility of LD measurements in healthy volunteers, with (a) Bland-Altman analysis of agreement (bias 0.0043 a.u, solid line; 95% LoAs ±0.028 a.u., dashed lines) and (b) raw data scatterplots

Fig. 5: Inter-reader variability of LD measurements in healthy volunteers, with (a) Bland-Altman analysis of agreement (bias 0.0014 a.u, solid line; 95% LoAs ±0.030 a.u., dashed lines) and (b) raw data scatterplots

Fig. 6: Healthy volunteer prandial stress studies with post-prandial changes in (a) PV flow, (b) LD and (c) correlation between changes in PV flow and LD

Fig. 7: Liver Deformation in healthy volunteer controls (■) and patients with cirrhosis (△)

Figure

Figures:

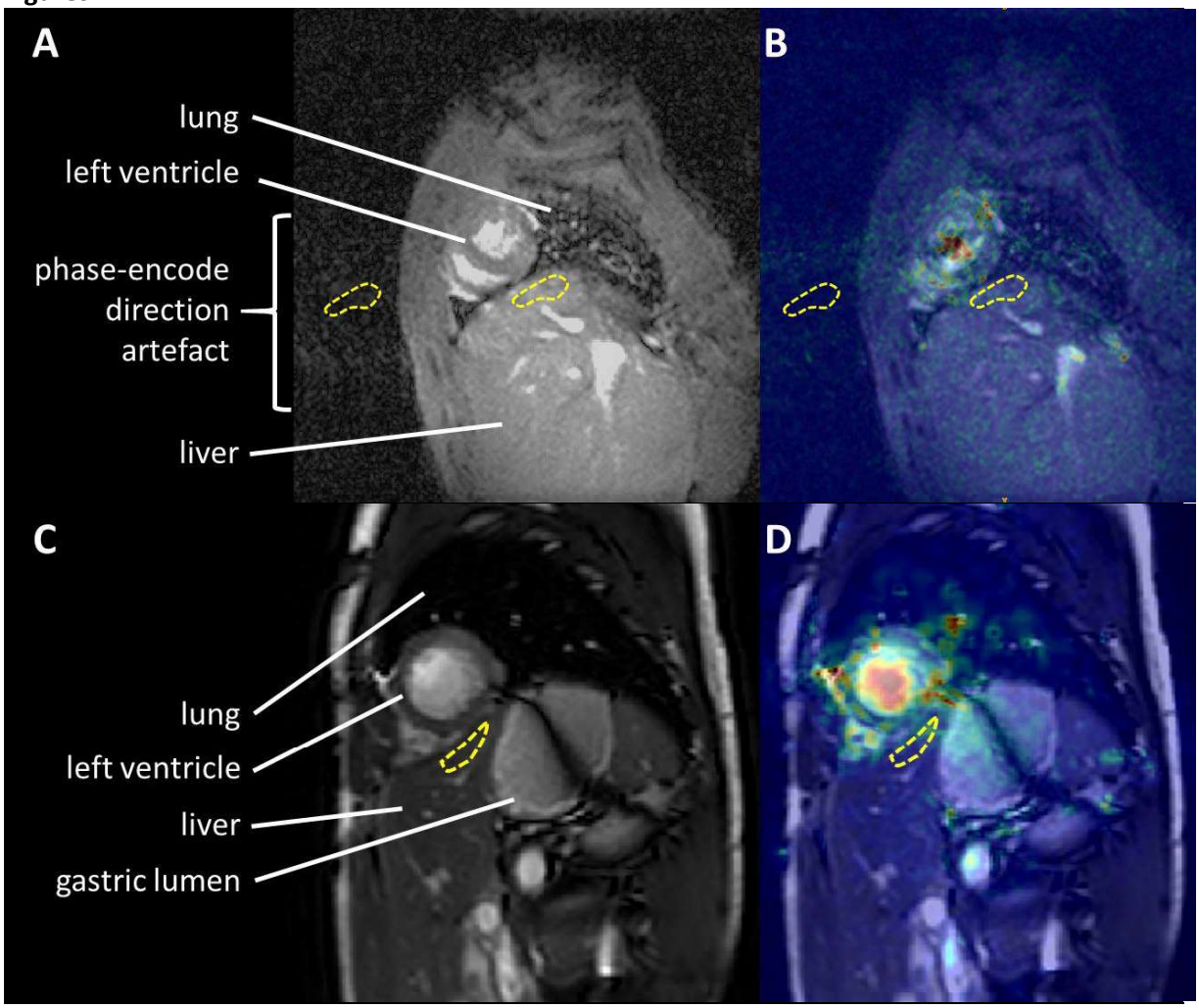

Figure 1

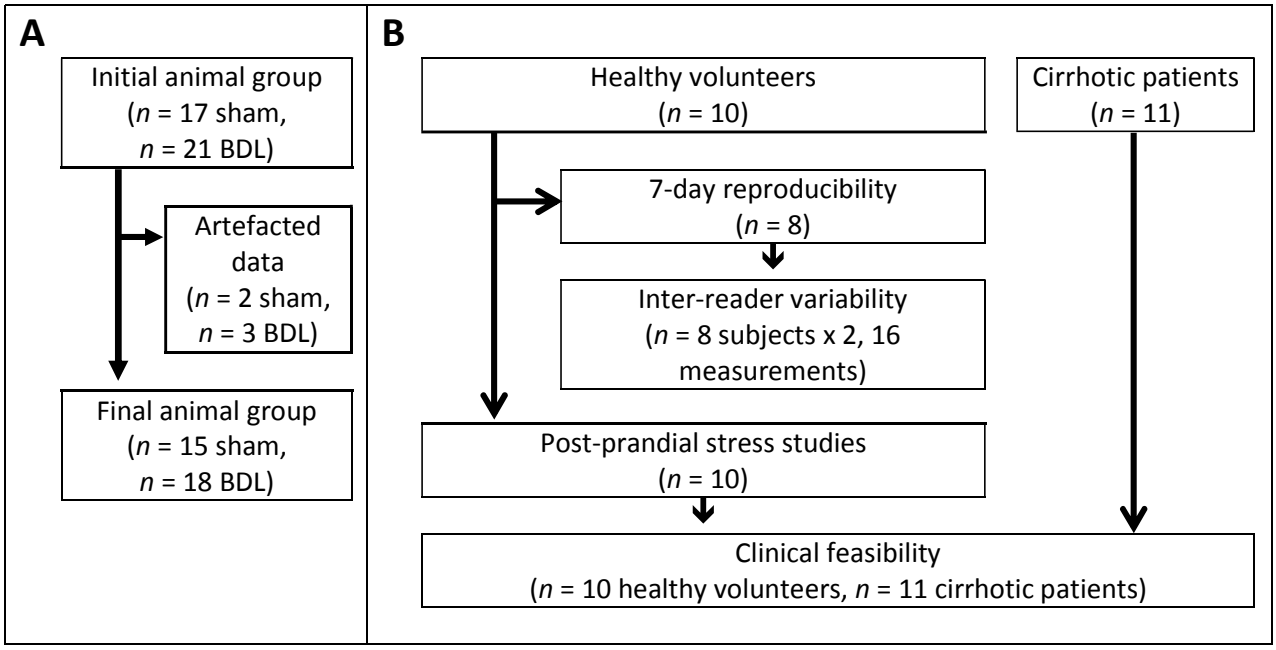
A
Initial animal group
(n = 17 sham,
n = 21 BDL)
Artefacted
data
(n = 2 sham,
n = 3 BDL)
Final animal group
(n = 15 sham,
n = 18 BDL)
B
Healthy volunteers
(n = 10)
Cirrhotic patients
(n = 11)
7-day reproducibility
(n = 8)
Inter-reader variability
(n = 8 subjects x 2, 16
measurements)
Post-prandial stress studies
(n = 10)
Clinical feasibility
(n = 10 healthy volunteers, n = 11 cirrhotic patients)

Figure 2

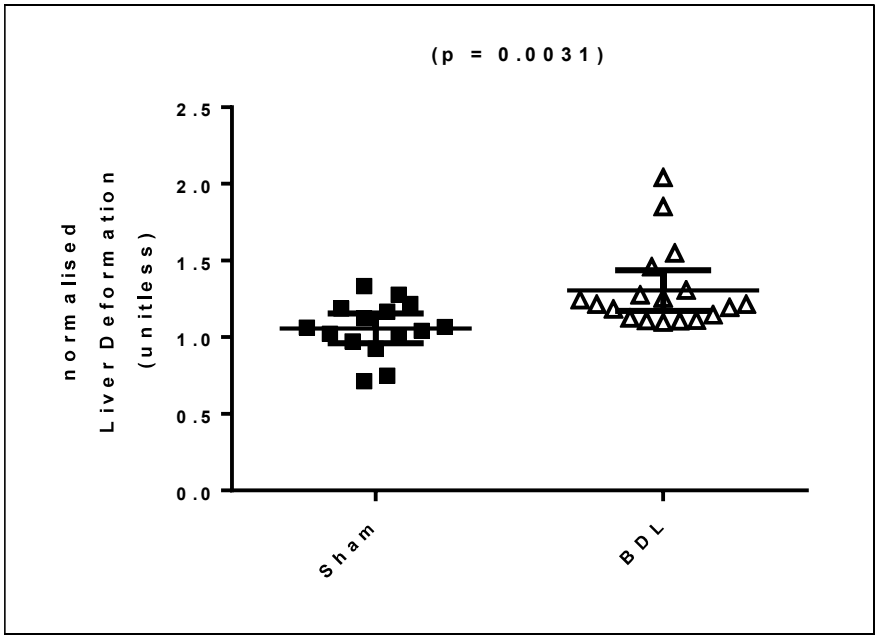
(p = 0.0031)
normalised Liver Deformation (unitless)
2.5
2.0
1.5
1.0
0.5
0.0
Sham
BDL

Figure 3

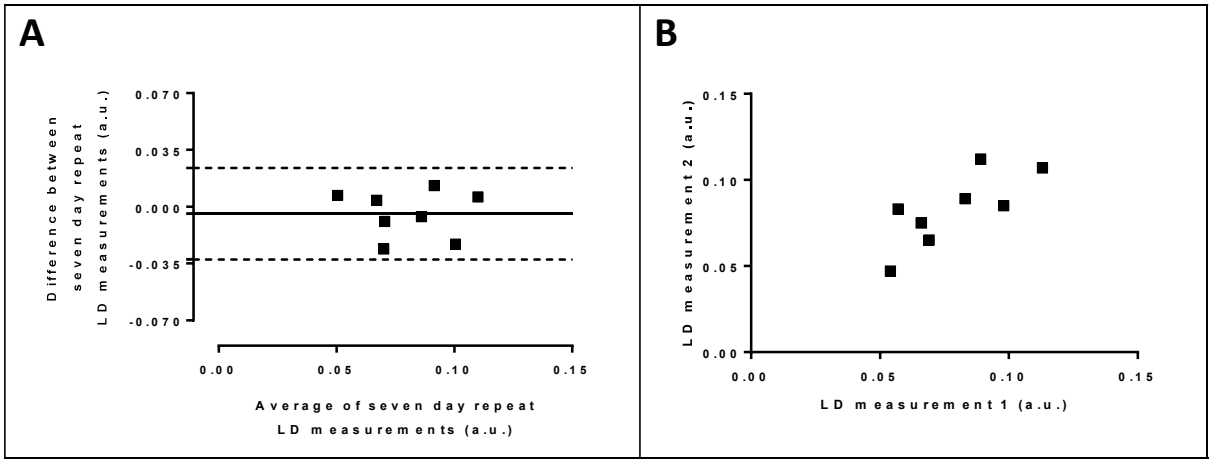
A
Difference between seven day repeat LD measurements (a.u.)
0.070
0.035
0.000
-0.035
-0.070
0.00
0.05
0.10
0.15
Average of seven day repeat LD measurements (a.u.)
B
LD measurement 2 (a.u.)
0.15
0.10
0.05
0.00
0.00
0.05
0.10
0.15
LD measurement 1 (a.u.)

Figure 4

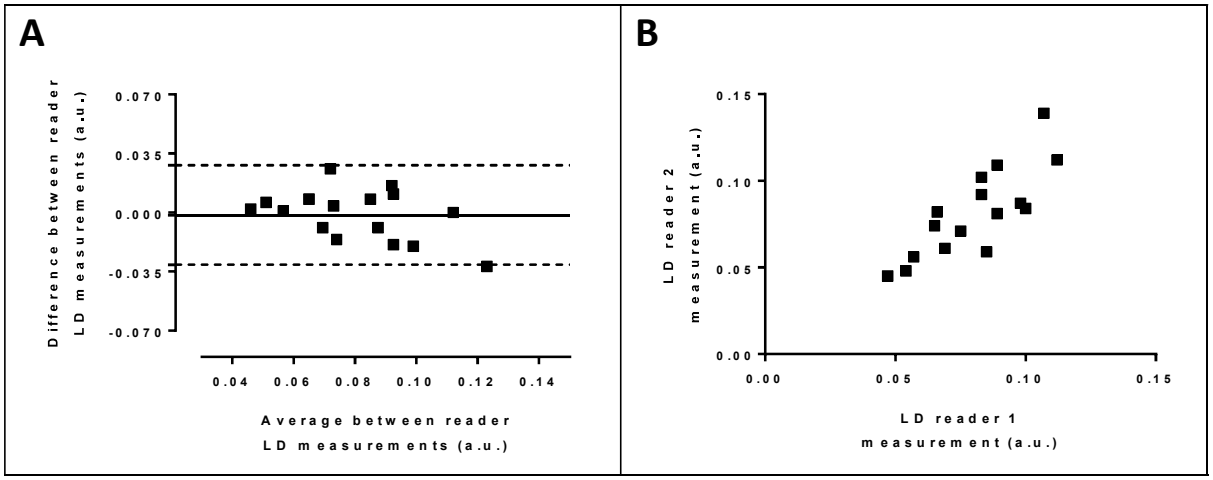
A
Difference between reader LD measurements (a.u.)
0.070
0.035
0.000
-0.035
-0.070
0.04
0.06
0.08
0.10
0.12
0.14
Average between reader LD measurements (a.u.)
B
LD reader 2 measurement (a.u.)
0.15
0.10
0.05
0.00
0.00
0.05
0.10
0.15
LD reader 1 measurement (a.u.)

Figure 5

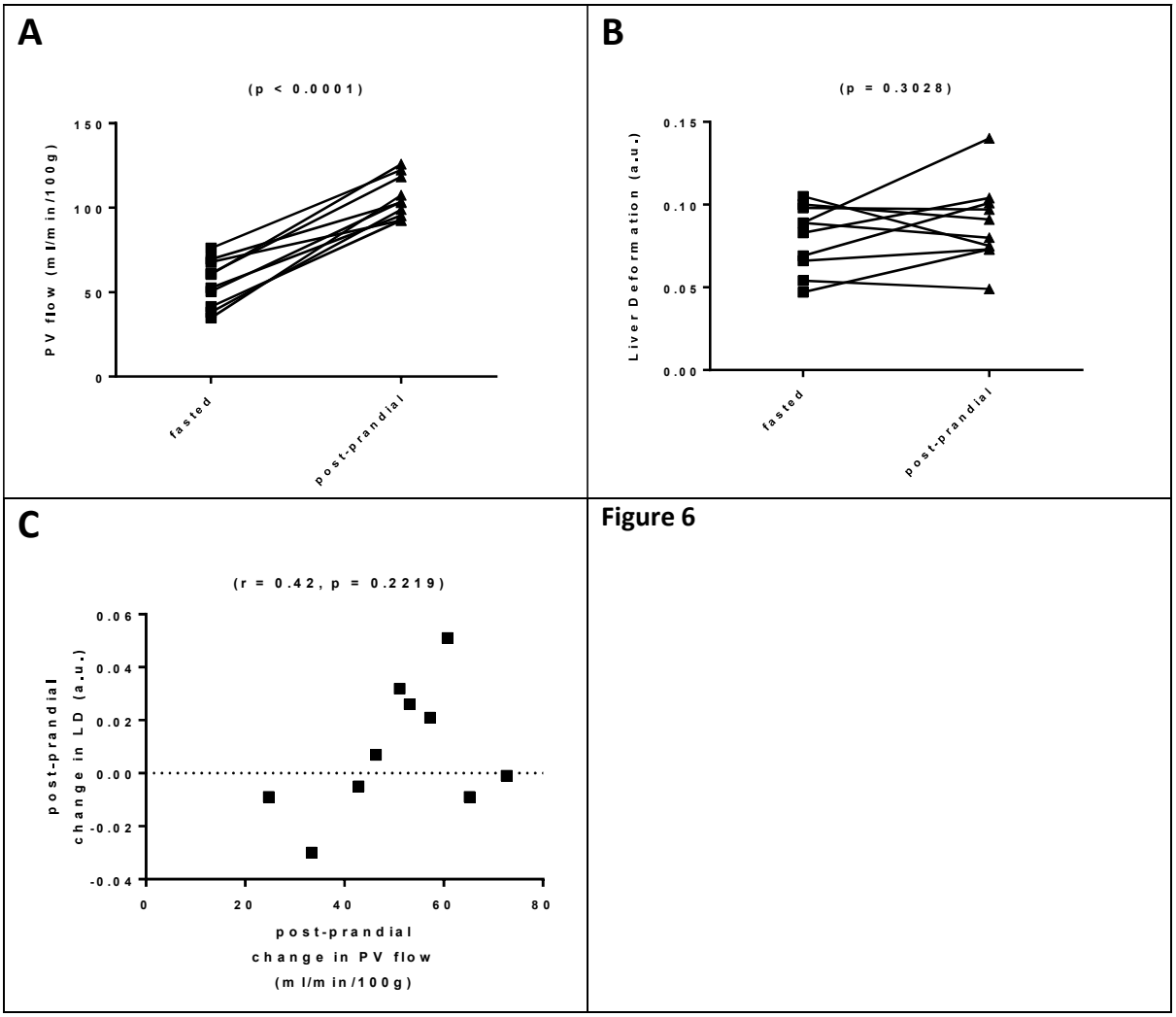
A
(p < 0.0001)
PV flow (ml/min/100g)
150
100
50
0
fasted
post-prandial
B
(p = 0.3028)
Liver Deformation (a.u.)
0.15
0.10
0.05
0.00
fasted
post-prandial
C
(r = 0.42, p = 0.2219)
post-prandial change in LD (a.u.)
0.06
0.04
0.02
0.00
-0.02
-0.04
0
20
40
60
80
post-prandial change in PV flow (ml/min/100g)

Figure 6

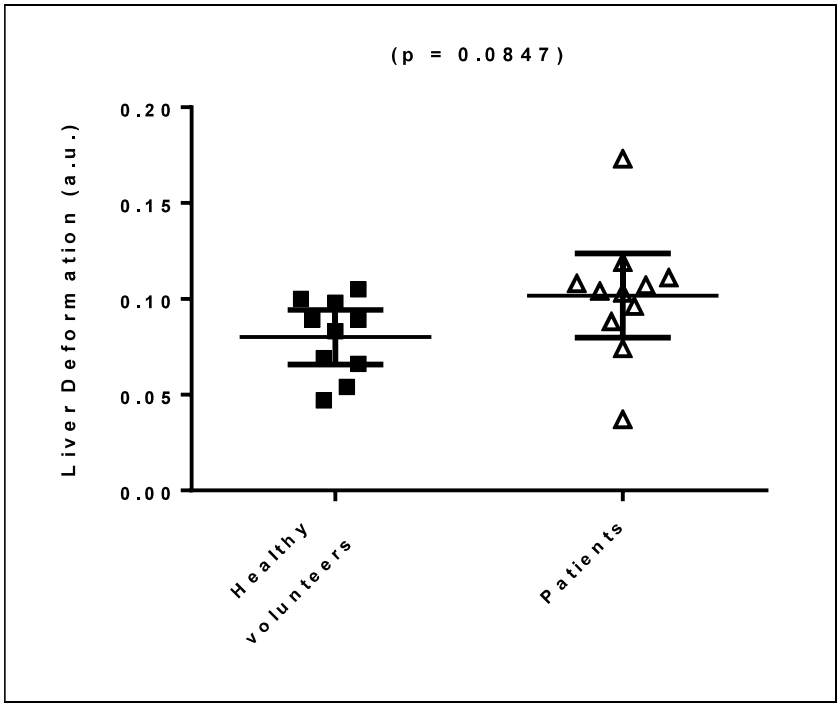
(p = 0.0847)
Liver Deformation (a.u.)
0.20
0.15
0.10
0.05
0.00
Healthy volunteers
Patients

Figure 7

Table

Tables:

	Preclinical (9.4T)		Clinical (3.0T)	
	Anatomical planning images (GE)	Cardiac cine MRI (GE)	Anatomical planning images (SSFP)	Cardiac cine MRI (GE)
TR/TE (milliseconds)	8.2/5.6	7.5/1.2	2.47/1.23	3.40/1.70
Flip angle (˚)	20	15	45	45
Matrix size (pixels)	128 x 128	128 x 64	352 x 352	256 x 256
Field-of-view (mm)	80 x 80	40 x 40	350 x 350	320 x 320
Spatial resolution (mm^2)	0.625 x 0.625	0.313 x 0.625	0.994 x 0.994	1.25 x 1.25
Slice thickness (mm)	2	1	5	8
Slice gap (mm)	4.5	0	5.5	8
Cardiac cycle phases	-	≥20	-	30

(GE – gradient echo, SSFP – steady-state free precession)

Table 1: Sequence parameters

	RAT (nLD)		HUMAN (LD)	
	MEAN±SE	P-VALUE[†]	MEAN±SE	P-VALUE[†]
Control group[‡]	1.058±0.045	-	0.080±0.0063	-
Post-prandial stress	-	-	0.088±0.0078	0.3028
Disease group[††]	1.304±0.062	0.0031*	0.102±0.0099	0.0847

([†]from comparison with control group data; [‡] sham-operated rats/healthy volunteers; [††]BDL rats/patients with cirrhosis; *P<0.05)

Table 2: nLD/LD measurements by study group

Response to reviewer comments

Graphical Abstract

Cardiac-induced liver deformation as a measure of liver stiffness using dynamic imaging without magnetisation tagging – preclinical proof-of-concept, clinical translation, reproducibility and feasibility in patients with cirrhosis

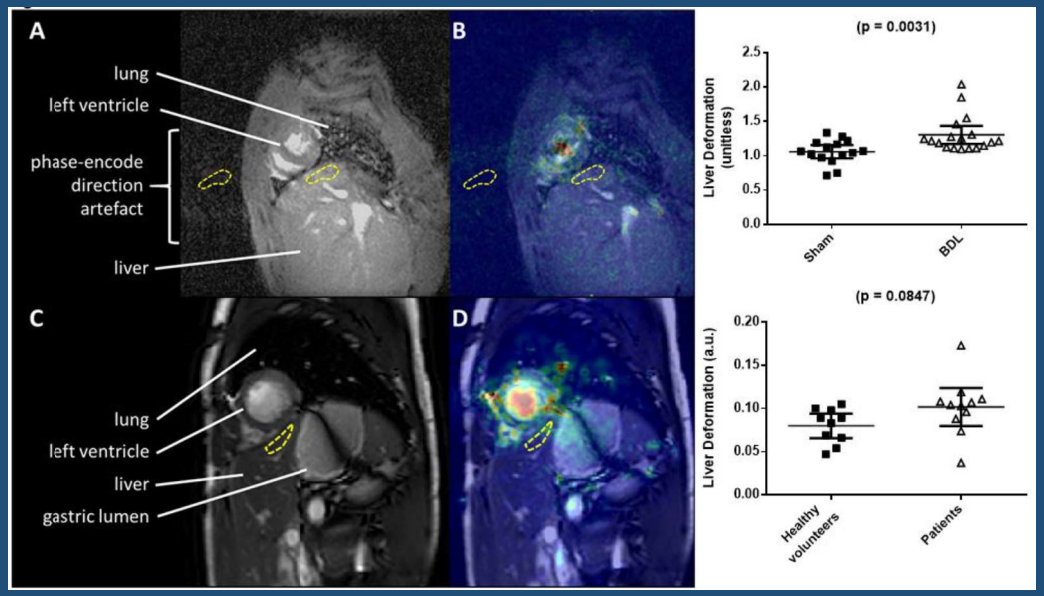

Liver deformation was higher in cirrhotic rats (p=0.0031), reproducible in healthy volunteers and feasible but not significantly different in a cirrhotic patients (p=0.0847).

Chouhan MD et al; 2021. DOI:

Abdominal Radiology
The Official Journal of the Society of Abdominal Radiology www.abdominalradiology.org